Journal of Applied Polymer Science

Synthesis and self-assembly study of zwitterionic amphiphilic derivatives of chitosan

Hellen Franciane Gonçalves Barbosa,[1] Aline Margarete Furuyama Lima,[1] Sebastião Roberto Taboga,[2] Júlio Cesar Fernandes,[3] Vera Aparecida de Oliveira Tiera,[1] Marcio José Tiera[1]

[1]Departamento de Química e Ciências Ambientais, Universidade Estadual Paulista, São Paulo, Brazil
[2]Departamento de Biologia, Universidade Estadual Paulista, São Paulo, Brazil
[3]Orthopedic Research Laboratory, Hôpital du Sacré-Cœur de Montreal, Université de Montreal, Montreal, Canada
Correspondence to: M. J. Tiera (E-mail: mjt@ibilce.unesp.br)

ABSTRACT: New zwitterionic derivatives of chitosan (CH) were synthesized through the Michael addition reaction of 1-(3-sulfopropyl)-2-vinylpyridine hydroxide (SPP) with primary amines of deacetylated CHs (with weight-average molecular weights of 46 and 216 kDa) to obtain SPP-substituted CHs. The hydrophilic derivatives were subsequently modified with 2.1, 4.6, and 9.7% of dodecyl groups [degree of substitution by dodecyl groups (DS_{Dod})]. The SPP-substituted CH derivatives were characterized by ^{1}H-NMR, Fourier transform infrared spectroscopy, and gel permeation chromatography. Aqueous solutions of SPP-substituted CH samples remained clear, independently of the pH ($3.0 < pH < 12.0$). The self-association study of the amphiphilic derivatives was performed in aqueous buffered solution at pH 5.0 and 7.4, and the critical aggregation concentration values varied from 5.6×10^{-3} to 0.02 g/L. The measurements of dynamic light scattering and ζ potentials showed that the self-assembly behavior was dependent on the pH and DS_{Dod}. At pH 7.4, the measured ζ potentials were near zero, and colloidal stability was provided by the hydrated zwitterionic shell of the aggregates. Transmission electron microscopy revealed spherelike microsized particles of broad distribution. The amphiphilic SPP-substituted CH samples were shown to be nontoxic with a 3-(4,5-dimethylthiazol-2-yl)-2,5-diphenyltetrazolium bromide assay performed with HeLa cells. The remarkable water solubility and nontoxicity displayed by the new SPP-substituted CH derivatives showed promising properties for the design of CH-based biomaterials and nanoparticles. © 2016 Wiley Periodicals, Inc. J. Appl. Polym. Sci. **2016**, *133*, 44176.

KEYWORDS: biopolymers and renewable polymers; colloids; drug-delivery systems; polysaccharides; self-assembly

Received 2 February 2016; accepted 10 July 2016
DOI: 10.1002/app.44176

INTRODUCTION

Amphiphilic derivatives of chitosan (CH) have received great attention in the literature because of their functional properties and potential applications as gene-, drug-, and protein-delivery vehicles.[1] The self-assembly of these systems is driven by hydrophobic groups linked to the CH backbone; this gives rise to the intramolecular and intermolecular interactions responsible for the formation of nanosized aggregates, whose properties depend on the degree of substitution, polymer concentration, temperature, and ionic strength.[2] The control of the hydrophilic/hydrophobic balance enables the formation of polymeric micelles for carrying a variety of drugs, such as those having antitumor activity,[3–7] hormones,[8] and plasmidial DNA.[9–11] The synthesis may be performed through nucleophilic attacks on the free amine and hydroxyl groups of the glucopyranose ring. However, substitution reactions on the hydroxyl groups require a sequence of protection/deprotection steps to obtain derivatives with a well-defined structure.[12,13]

A wide range of procedures have been used to provide the required properties of CH derivatives, and they involve the control of the degree of acetylation and the weight-average molecular weight (M_w), followed by chemical derivatization with anionic[14] and cationic[15,16] groups and polymers.[17] The insertion of hydrophilic groups and polymers, such as carboxylic, polycaprolactone,[18] poly(ethylene glycol),[19] and others,[20] provides the advantage of enhancing the water solubility and preventing protein adsorption, a desirable property in the design of CH-based drug-delivery systems. Like poly(ethylene glycol),

Additional Supporting Information may be found in the online version of this article.

Table I. Amphiphilic Derivative Characterization, Compositions, Molecular Weights, Polydispersities, and CACs

	Composition					CAC (g/L × 10^3)[b]		
Derivative	DS_{SPP} (mol %)[a]	D_{CHO}/SPP-substituted CH (molar ratio in feed)	DS_{Dod} (mol %)[a]	M_w (g/mol)	M_w/M_n	pH 5.0	pH 6.2	pH 7.4
CH_L	—		—	4.6×10^4	5.0			
SPP_{36}-CH_L	36.0		—	3.2×10^4	2.5			
SPP_{36}-CH_L2	36.0	0.04	2.1	—	—	16.9	14.7	11.3
SPP_{36}-CH_L5	36.0	0.06	4.6	—	—	15.4	13.3	12.2
SPP_{36}-CH_L10	36.0	0.12	9.7	—	—	9.1	8.6	7.9
CH_M	—		—	2.05×10^5	3.5			
SPP_{50}-CH_M	45.7		—	2.16×10^5	4.9			
SPP_{50}-CH_M2	45.7	0.04	2.1	—	—	9.1	6.5	5.6

M_n, number-average molecular weight.
[a] Determined by ^{1}H-NMR.
[b] Determined by pyrene fluorescence at 25 °C with an ionic strength of 150 m*M*.

zwitterionic groups provides a highly hydrated layer to nanoparticles and interfaces; this improves the biocompatibility of nanodevices and surfaces.[21]

The synthesis of zwitterionic derivatives of CH has been devised with different procedures, such as conjugation with succinic anhydride,[22–24] the reaction with 2-chloro-2-oxo-1,3,2-dioxaphospholane,[25] the Atherton–Todd reaction with dicholinyl phosphite dichloride,[26] the Michael addition reaction of 2-methacryloyloxyethyl phosphorylcholine,[27,28] and the reductive amination reaction.[29]

Zwitterionic derivatives of CH have been exploited as possible carriers for antitumor drugs, such as camptotecin[30] and doxorubicin,[31] but studies focusing on the effect of composition on the self-assembly behavior have been limited. We describe here the effect of the hydrophobe content, pH, and M_w on the self-assembly of zwitterionic derivatives of CH. The derivatives were obtained through the Michael addition reaction of 1-(3-sulfopropyl)-2-vinylpyridine hydroxide (SPP) with a fully de-*N*-acetylated CH; this was followed by reductive alkylation with dodecylaldehyde (D_{CHO}). The derivatives were characterized by ^{1}H-NMR, gel permeation chromatography (GPC), Fourier transform infrared (FTIR), and turbidimetry. Their associative behavior in aqueous solutions was studied with fluorescence spectroscopy, dynamic light scattering (DLS), and ζ-potential measurements. The cytotoxicity of the derivatives was evaluated to confirm their nontoxic nature.

EXPERIMENTAL

Materials

Commercially available CH (degree of deacetylation = 85%), used as the starting material, was purchased from Polymar Co. (Fortaleza, Ceará, Brazil) and deacetylated as described previously.[29] Sodium acetate, acetic acid, sodium hydroxide, sodium chloride, and ethanol were purchased from Synth (Diadema, São Paulo, Brazil). Sodium cyanoborohydride, deuterium chloride (35%) in deuterium oxide, deuterium oxide, D_{CHO}, sodium dihydrogen phosphate monohydrate, SPP, and *N*,*N*-dimethylformamide were purchased from Sigma-Aldrich Chemical Co. (Brazil). Water was deionized with a Gehaka water purification system. Spectra/Pore membranes (Spectrum) were used for dialysis. All solvents were reagent grade and were used as received.

Preparation of the Amphiphilic CHs

The derivatives were synthesized as reported previously[32] with highly deacetylated CH samples denoted as CH_L (46 kDa) and CH_M (216 kDa). The procedure is illustrated below for the synthesis of SPP_{50}–CH_M10, a derivative containing 46% of SPP and 10% of dodecyl groups. A solution of SPP (8.0 g, 37.2 mmol) in water (20 mL) was added dropwise to a solution of deacetylated CH (3.0 g, 18.6 mmol monosaccharide residue) in aqueous acetic acid (150 mL, 1 wt %) at room temperature. The solution was stirred for 24 h at 50 °C. Then, the pH of the reaction mixture was adjusted to 9.0 by the addition of aqueous sodium bicarbonate, and the reaction mixture was dialyzed (membrane molecular weight cutoff = 2000 g/mol) against water for 5 days. The derivative SPP_{50}–CH was isolated by lyophilization. The zwitterionic derivative SPP_{50}–CH (0.8 g) was solubilized in a mixture of 90 mL of 2% acetic acid and 60 mL of ethanol.[2] The pH was adjusted to 5.0 with a sodium hydroxide solution, and while the reaction mixture was stirred, 0.07 mL of D_{CHO} dissolved in 10 mL of ethanol was added dropwise to the mixture. The reaction mixture was continuously stirred for 24 h at room temperature, and sodium cyanoborohydride was added to a ratio of 3:1 $NaCNBH_3$–glucosamine) after the first hour. Thereafter, the reaction mixture was dialyzed (membrane molecular weight cutoff = 2000 g/mol), first against water for 2 days, then against aqueous sodium hydroxide (0.05 *M*) for 1 day, and finally against water for 3 days. The derivative was recovered by lyophilization. The derivatives were subsequently purified in a Soxhlet system with chloroform to remove nonreacted D_{CHO}. The derivatives were characterized by ^{1}H-NMR, FTIR spectroscopy, and GPC measurements. Other SPP-grafted CHs were prepared under identical conditions except for the different initial dodecyl molar ratios, which are shown in Table I. The overview of the synthesis is shown in Scheme 1.

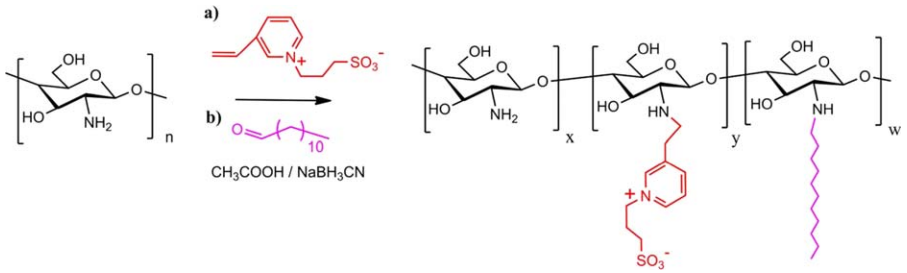

Scheme 1. Synthesis of the amphiphilic derivatives of CH: (a) Michael addition and (b) reductive amination reactions. [Color figure can be viewed in the online issue, which is available at wileyonlinelibrary.com.]

^{1}H-NMR Measurements

Samples were prepared by the dissolution of 10 mg of the derivatives in 1.0 mL of deuterium oxide; this was followed by the addition of 10 μL of deuterium chloride solution in deuterium oxide and subjected to magnetic stirring until solubilization was complete. ^{1}H-NMR measurements of the deacetylated CH and its derivatives were performed on a 500-MHz Bruker spectrometer (ARX-500) at 70 °C.

Attenuated Total Reflectance/FTIR Measurements

The chemical structures of the derivatives were characterized with an attenuated total reflectance/FTIR spectrophotometer (PerkinElmer, Spectrum 100). Each spectrum was acquired in transmittance mode by the accumulation of 50 scans with a resolution of 4 cm^{-1} in the range 4000–600 cm^{-1}.

GPC Analysis

GPC measurements were performed with an LC-20 Shimadzu liquid chromatograph (Shimadzu, Japan) equipped with a refractive-index detector (model RID-10) with OHpak SB-803 HQ and OHpak SB-805 HQ columns (Shodex) and pullulan standards from 805 to 6.2 kDa (Figure S1 in the Supporting Information). A mixture of acetic acid (0.3 *M*) and sodium acetate (0.2 *M*, pH 4.5) was used as the mobile phase at a flow rate of 0.8 mL/min at 35 °C. Solutions were prepared for GPC analysis by dissolution of the polymer in an acetic acid (0.3 *M*)/sodium acetate (0.2 *M*) buffer to achieve concentrations of between 0.5 and 1.0 mg/mL. The polymer solutions were stirred for 3 days and then filtered through 0.45-μm membranes before analysis.

Turbidity Measurements

The solubility of the different derivatives was investigated by the monitoring of the change in the transmittance of a given polymer solution as a function of the pH. The transmittance was measured at 550 nm. To measure the transmittance as a function of the pH, solutions at various pH values of CH and their derivatives (1.0 mg/mL) were first dissolved in 0.10 mol/L acetic acid at pH 2.9. Then, the solution pH was adjusted to a desired value through the addition of aliquots of 25 μL of sodium hydroxide (0.5 *M*). The solution pH was measured with a pH meter (Digimed pH meter with a DME-CF1 glass pH electrode). The transmittance values were recorded on a Cary 100 ultraviolet–visible spectrophotometer equipped with a Peltier 1 × 1 system, and measurements were taken after 2 min of magnetic stirring.

Self-Aggregation Study

The self-association of the amphiphilic derivatives was evaluated at 25.0 ± 0.1 °C with a Hitachi 4500 fluorescence spectrometer (Hitachi, Japan). Fluorescence experiments with pyrene as a probe were performed at 25 °C with acetic acid/sodium acetate (pH 5.0) and phosphate-buffered saline (pH 6.2 and 7.4) buffers at an ionic strength of 150 m*M*. One microliter of a stock solution of pyrene (1 m*M*) in methanol was added to a quartz cuvette, and the solvent was removed by the blowing of N_2. To each of these pyrene-containing cuvettes was added 2 mL of buffer; this was followed by sonication. Measured amounts (10 μL) of concentrated stock solutions of the derivatives (2.0 g/L) were then added to buffered aqueous solutions of pyrene (5.0×10^{-7} *M*) under magnetic stirring, and fluorescence spectra were recorded after each addition. The ratio of the fluorescence intensities of peaks I (372.4 nm) and III (384 nm) of the emission spectrum of pyrene (the I_1/I_3 ratio) as a function of the polymer concentration was used to evaluate the polarity of the local environment and to determine the critical aggregation concentration (CAC). Pyrene was excited at 310 nm, and its emission was recorded from 350 to 650 nm. CACs were determined with the beginning of the decline of the I_1/I_3 as criteria, as described previously.[33,34]

Transmission Electron Microscopy (TEM)

Solutions of the derivatives were prepared at concentrations of 0.01 and 1.0 mg/mL at pH 5.0 and an ionic strength of 150 m*M*. One drop of the particle solution was deposited on the copper grid (carbon-coated copper grid, 200 mesh). The grids were allowed to dry for 30 min and poststained with uranyl acetate, and then, the images were recorded with a Leo Zeiss 906 transmission electron microscope operating at 80 kV.

DLS

DLS experiments were performed on a Zetasizer Nano-ZS90 with an He–Ne laser (λ = 633 nm) and a 90° scattering angle. The temperature was 25 °C unless otherwise stated. The measurements were performed at concentrations of 0.5 and 1.0 mg/mL at pH 7.4 in 50 m*M* phosphate buffer with an ionic strength of 150 m*M*. The measurements were performed in duplicate with three accumulations for each solution, and the average sizes were used. ζ potential measurements of the particles were performed in the range 0.2–1.5 mg/mL at pH values of 5.0 and 7.4.

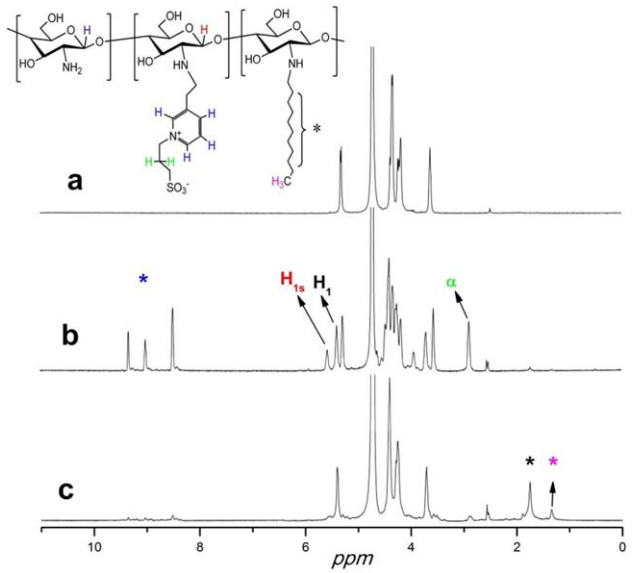

Figure 1. ^{1}H-NMR spectra of CH and its derivatives in deuterium oxide/deuterim chloride at 70 °C: (a) CH_M, (b) SPP_{36}–CH_L, and (c) SPP_{36}–CH_L10. [Color figure can be viewed in the online issue, which is available at wileyonlinelibrary.com.]

Cell Viability

HeLa and L929 fibroblast cells were cultured in Dulbecco's modified Eagle's medium supplemented with 10% fetal bovine serum and 1% penicillin–streptomycin in a 5–95% CO_2–O_2 atmosphere at 37 °C. Cells were seeded in triplicate in 96-well culture plates at a density of approximately 1×10^4 cells/mL in 200 μL of cell culture medium per well. The cells were cultured for 24 h at 37 °C. Thereafter, they were exposed to CH and its derivatives (0.50 and 1.5 g/L) and then incubated for a period of 24 h. The cell viability was evaluated with a 3-(4,5-dimethylthiazol-2-yl)-2,5-diphenyltetrazolium bromide (MTT) colorimetric assay, as previously described.[29] The absorbance was measured at 570 nm with an ELX 808 universal microplate reader (Bio-Tek Instruments, Inc.).

RESULTS AND DISCUSSION

Synthesis and Characterization of the Zwitterionic CHs

Although other methods are available for obtaining zwitterionic CHs, we chose the Michael addition reaction because of the simplicity and selectivity of this method. The transformation was carried out from a fully deacetylated CH with a degree of deacetylation of 99.9%, as determined from the ^{1}H-NMR spectrum [Figure 1(a)]. The fully deacetylated CH was treated first with SPP monomer; this was followed by the reductive amination reaction with D_{CHO} (Scheme 1). The ^{1}H-NMR spectrum of the SPP-modified CH (SPP_{36}–CH_L) exhibited new characteristic signals of the grafted zwitterionic group, the first at δ = 2.88 ppm, which was attributed to the resonance of the methylene protons of the SPP group $^-O_3SCH_2CH_2CH_2-$ [α signal; Figure 1(b)], and signals at δ = 8.4–9.4 ppm, which corresponded to the resonances of the protons linked to the pyridine ring [Figure 1(b)]. The attachment of the SPP groups to the CH backbone produced new signals in the ^{1}H-NMR spectrum of CH; this was attributed to the anomeric proton (δ 5.55 ppm) and the proton linked to the C2 of the glucosamine unit (δ 3.55 ppm). A downfield shift, from a δ of 5.34 to a δ of 5.55 ppm, was observed for the anomeric proton, whereas the signal corresponding to the proton linked to C2 shifted to 3.70 ppm. The attachment of dodecyl groups was evidenced by the characteristic signals at δs of 1.35 and 1.75 ppm, which corresponded to the terminal —CH_3 and methylene protons of the hydrocarbon chain, respectively [Figure 1(c)].

The degree of substitution by SPP (DS_{SPP}) was determined from the areas of the signal at a δ of 2.88 ppm, which was attributed to the resonance of the methylene group $O_3SCH_2CH_2CH_2-$ [signal α(I_{CH2}); Figure 1(b)], and of the signals due to the anomeric protons of SPP-substituted (δ = 5.34–5.55 ppm) and unsubstituted glucosamine residues H1s and H1, respectively [Figure 1(b)] with eq. (1):

$$DS_{SPP} = \frac{I_{CH_2}/_2}{(I_{H_1} + I_{H_{1S}})} \quad (1)$$

The degree of substitution by dodecyl groups (DS_{Dod}) was determined from the areas of the signal at a δ of 1.35 ppm (I_{CH3}) and the signals due to the anomeric protons (δ = 5.34–5.55 ppm) with eq. (2):

$$DS_{Dod} = \frac{I_{CH_3}/3}{I_{H_1} + I_{H_{1S}}} \quad (2)$$

The derivatives containing 36.0 and 45.7 mol % of zwitterionic groups (Table I) were modified with increasing proportions of dodecyl groups through the variation of the ratio of glucosamine units to D_{CHO} in the feed; this provided derivatives with 2.1, 4.6, and 9.7 mol % of dodecyl groups (Figure S2, Supporting Information). The FTIR spectroscopy provided further evidence for the successful incorporation of SPP and dodecyl moieties onto the CH backbone. The IR spectra of the deacetylated CH, SPP_{36}–CH_L2, and SPP_{36}–CH_L10 samples (Figure 2) present typical traces of the SPP and dodecyl groups with bands at 720–770 and 1040 cm^{-1}, which corresponded to the C—H stretching of the aromatic ring and the stretching of the S=O bond of the SPP group. The appearance of two bands at 2850 and 2929 cm^{-1} were also attributed to the C—H stretching of dodecyl chains and confirmed successful grafting.

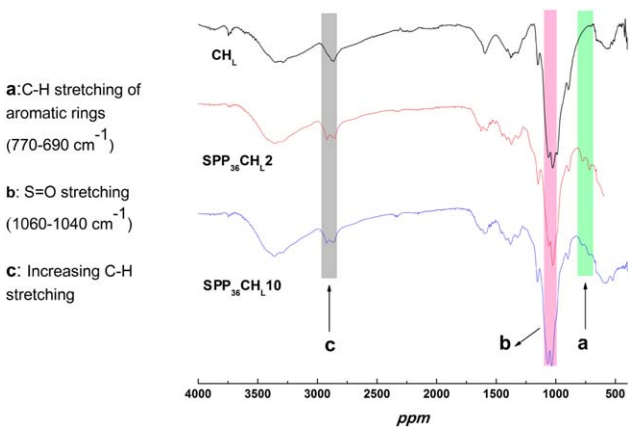

Figure 2. IR spectra of deacetylated CH (CH_L) and its zwitterionic derivatives SPP_{36}–CH_L2 and SPP_{36}–CH_L10. [Color figure can be viewed in the online issue, which is available at wileyonlinelibrary.com.]

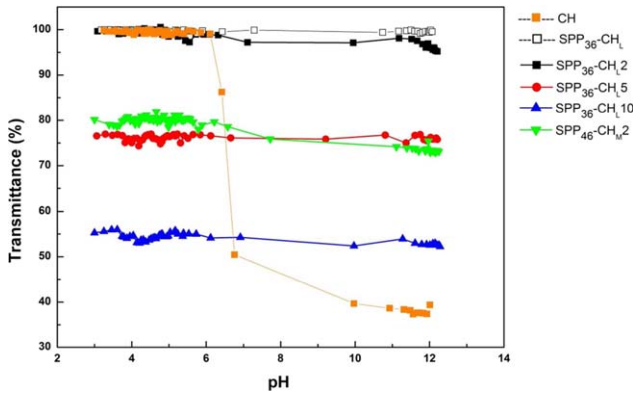

Figure 3. Transmittance of solutions of CH and SPP-modified amphiphilics at $\lambda = 566$ nm (polymer concentration = 1.0 g/L). [Color figure can be viewed in the online issue, which is available at wileyonlinelibrary.com.]

In the first step of the reaction, the insertion of the zwitterionic groups (SPP-substituted CH) was performed in an acid medium at 50 °C, and as shown in Table I, GPC analysis confirmed that the molecular mass of the SPP_{36}–CH_L derivative decreased in comparison with the starting CH (CH_L). However, the molar masses of both hydrophilic derivatives (SPP_{36}–CH and SPP_{50}–CH) remained near those obtained for the starting CHs. We could rationalize this by taking into account the fact that the insertion of these groups could induce conformational changes and, thus, affect the retention time.[35] Moreover, as shown in Table I, the M_w distribution was also affected, and the polydispersities of both hydrophilic derivatives decreased because of the extensive dialysis process. The subsequent step, the reductive amination reaction with D_{CHO}, was performed under mild conditions, and significant degradation was not expected. To assess the effect of the zwitterionic group on the solubility of the amphiphilics, we performed turbidity measurements by monitoring changes in the transmittance of solutions of CH and its derivatives as a function of pH. As exemplified in Figure 3, the insertion of zwitterionic groups increased the solubility of SPP_{36}–CH_L (32 kDa) and SPP_{50}–CH_M (216 kDa) over the entire range of pH, whereas the transmittance for the solution of CH_M (pKa ≈ 6.2) decreased sharply at pH values greater than 6.2. For the more substituted amphiphilic derivatives (SPP_{36}–CH_L5 and SPP_{36}–CH_L10), the solutions' transmittances were decreased to about 75 and 55%; however, they remained constant and partially transparent over the entire range of pHs. This denoted an increasing aggregation as DS_{Dod} increased from 2 to 10 mol %. Although the same degrees of substitution were obtained for SPP_{50}–CH_M2 and SPP_{36}–CH_L2 ($DS_{Dod} \sim 2.0\%$), $SPP_{50}CH_M2$ exhibited a lower transmittance; this was attributed to its higher M_w, which indicated a more efficient aggregation. The effects of the degree of substitution and pH on the self-association of the derivatives were evaluated by means of fluorescence spectroscopy with pyrene as a probe, and they are discussed in the following section.

Amphiphilic Properties Probed by Pyrene Fluorescence

The self-association of the zwitterionic derivatives was studied in aqueous buffered solutions at pHs of 5.0, 6.2, and 7.4 with the I_1/I_3 ratios of peaks I (372.4 nm) and III (384 nm) of the vibronic bands of the emission spectra of pyrene (Figure 4).[28] All dodecylated derivatives exhibited aggregation in the concentration range of 0.005–0.02 g/L; this depended on their compositions (Table I). As the amphiphilics were polydisperse samples, the CAC reflected the beginning of the self-association process, and as shown in Figure 4 and Table I, the CAC values decreased as the dodecyl content and pH increased. It has been well documented that even at low pH, the nonmodified and hydrophobicized CHs aggregated; this depended on their M_w and degree of substitution values.[33,34,36] Moreover, this aggregation took place above a critical pH and was dependent on the degree of acetylation.[37] As shown in Figure 4, the hydrophilic derivatives (SPP_{36}–CH_L, 32 kDa, and SPP_{50}–CH_M, 216 kDa) exhibited no sign of aggregation, and the I_1/I_3 ratios remained around 1.9–2.0, even at concentration of 1.0 g/L (Figure S3, Supporting Information). This corroborated the data obtained with turbidity measurements (Figure 3). However, the introduction of even a small percentage of dodecyl groups (∼2%) was responsible for overcoming the electrostatic repulsion of charged amino groups and led to the formation of aggregates, whose probed polarities ($I_1/I_3 \approx 1.1$–1.2) were lower than those obtained with the cationic surfactant dodecyltrimethylammonium bromide (DTAB).[38] As the pH increased from 5.0 to 7.4, the CAC values decreased approximately 30%; this was attributed to the deprotonation of the amino groups. At pH 7.4, the electrostatic repulsion decreased, the intramolecular and intermolecular interactions were strengthened, and a more prominent aggregation was observed with the higher M_w derivative (216 kDa), SPP_{50}–CH_M2 (2% of dodecyl), whose CAC was 5.6×10^{-3} g/L. This result was consistent with the turbidity measurements and indicated that this derivative self-aggregated more efficiently

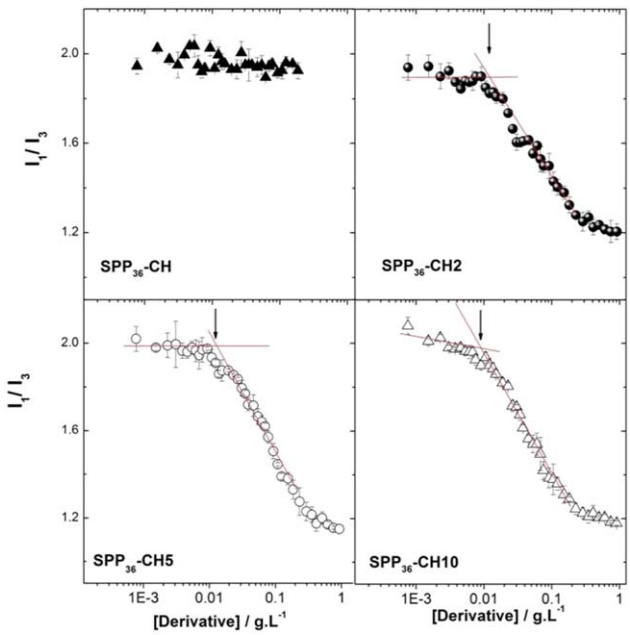

Figure 4. I_1/I_3 ratio versus the SPP_x–CH_y concentration at pH 7.4. [Color figure can be viewed in the online issue, which is available at wileyonlinelibrary.com.]

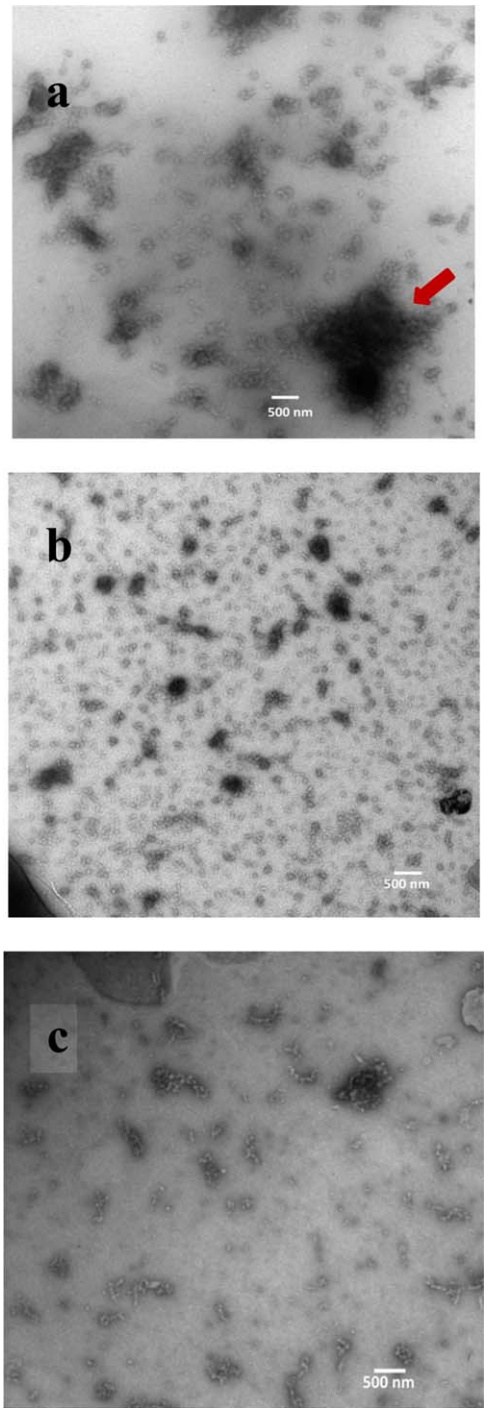

Figure 5. TEM images of (a) SPP_{36}–CH_L2 and (b) SPP_{50}–CH_M2 particles at 1.0 mg/mL and (c) SPP_{36}–CH_M10 at 0.01 mg/mL(pH 5.0, ionic strength = 150 m*M*). [Color figure can be viewed in the online issue, which is available at wileyonlinelibrary.com.]

than SPP_{36}–CH_L2, the lower M_w derivative grafted with 2% of dodecyl groups.

TEM, DLS, and ζ Potential Measurements

TEM measurements were taken to evaluate the shape and size of the aggregates. The TEM image of the SPP_{36}–CH_L2 microparticles at pH 5.0 and an ionic strength of 150 m*M* is shown in Figure 5(a). These particles were near spherical in shape with a wide size distribution and the formation of larger aggregates (red arrow), composed in some cases of smaller spheres. It was shown that the hydrodynamic diameter (D_h) of aggregates of hydrophobically modified CH increased from 130 to 300 nm as the M_w was increased from 5×10^3 to 2×10^5.[39] The authors postulated that with increasing M_w ($M_w > 40$ kDa), the rigidity of the CH chain favored the intermolecular self-association of the pendant hydrophobic groups with the formation of birds nestlike structures.[39] The images obtained for SPP_{50}–CH_M2 (205 kDa) showed spherelike micelles [Figure 5(b)]. However, as shown in Figure 5(c), for the most substituted derivative, SPP_{36}–CH_M10, at 0.01 mg/mL, several elongated and larger aggregates were observed. These aggregates may have been formed by bridges between the micellar aggregates[40] and could have been partially driven by hydrogen bonding and some crosslinking of the zwitterionic groups.

We performed DLS and ζ-potential measurements, aiming to evaluate the aggregates' size distribution and their dependence on the degree of substitution and pH. The data obtained at pH 7.4 and 5.0 as a function of the polymer concentration are shown in Figure 6(a–c). Overall, the aggregates' sizes obtained by DLS measurements were higher than those observed in the

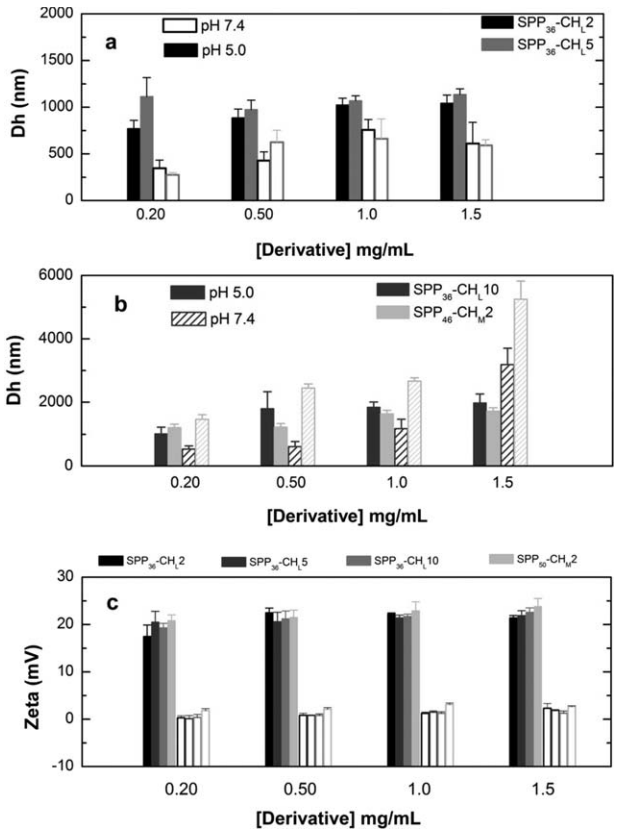

Figure 6. Sizes (D_h) of SPP_x–CH aggregates at pH 5.0 (filled bars) and pH 7.4 (open bars) as a function of concentration for (a) SPP_{36}–CH_L2 and SPP_{36}–CH_L5 and (b) SPP_{36}–CH_L10 and SPP_{50}–CH_L2. (c) ζ potentials at pH 5.0 (filled bars) and pH 7.4 (open bars). The data are presented as means and standard deviations ($n = 3$).

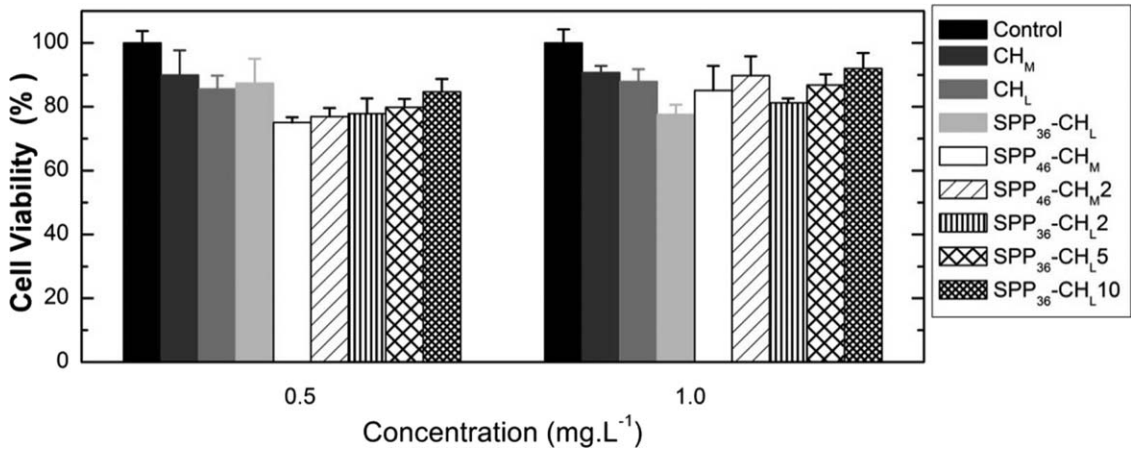

Figure 7. Impact of the CH derivative composition on the HeLa cell viability evaluated with the MTT assay after 24 h of incubation at 37 °C of the cells in the presence of the polymer (0.5 and 1.0 g/L).

TEM images because, in the latter case, dried aggregates were expected to present smaller dimensions.[41] The results are presented in two groups. The first group included the less substituted derivatives of low M_w [SPP_{36}–CH2 and SPP_{36}–CH5; Figure 6(a)], and the second included SPP_{36}–CH_L10 and SPP_{50}–CH_M2, the most substituted and the higher M_w derivative, respectively [Figure 6(b)].

At pH 7.4, the ζ potential was near zero [open bars in Figure 6(c)]; this indicated that the pK_a of the amino group was not significantly altered by the addition of the zwitterionic group. At neutral pH, both SPP_{36}–CH_L2 and SPP_{36}–CH_L5 exhibited smaller aggregate sizes [500–600 nm; opens bars in Figure 6(a)] than at pH 5.0. A similar pattern was also observed by Liu *et al.*,[43] when they were working on linoleic acid-modified CH; it could be explained by the reinforcement of the hydrophobic interactions as the degree of charging of the polymer chain decreased. This behavior suggested a well-defined core–shell structure[41,42] previously observed with hydrophobically modified CHs, which even at neutral pH did not exhibit phase separation.[42,43]

At pH 5.0, all of the derivatives were fully charged, and the ζ potentials remained around 20 mV [filled bars in Figure 6(c),] and aggregates of SPP_{36}–CH_L2 and SPP_{36}–CH_L5 doubled in size, exhibiting D_h values of 1000 nm [Figure 6(a)] with high polydispersities (polydispersity index = 0.4–0.7). We rationalized the higher D_h values at low pH by taking into account the fact that the repulsion between the charged amino groups led to more extended chain conformations and higher and more hydrated aggregates.[44] Moreover, as shown in Figure 6(a), the aggregates sizes increased only modestly in the concentration range studied (0.2–1.5 mg/mL); this was credited to a hydrophilic shell on the aggregate surface provided by the zwitterionic groups.

In contrast, at neutral pH, the aggregates sizes of SPP_{36}–CH_L10 increased abruptly with the polymer concentration, from 500 nm at 0.2 mg/mL to 3.0 μm at 1.5 mg/mL [Figure 6(b)]; this corroborated the data obtained with turbidity and the TEM measurements. A similar pattern was observed for SPP_{50}–CH_M2 (the higher M_w derivative); this produced the greatest sizes, which reached values of 2.0–5 μm. Because of its higher M_w, SPP_{50}–CH_L2 was more prone to exposing the longer chains to the hydrophilic shell, whereas for SPP_{36}–CH_L10, the high content of hydrophobic groups may have imposed their presence in the hydrophilic shell. In both cases, this drove the formation of larger aggregates.[42]

In Vitro Cytotoxicity Study

The cytotoxicity of CH and its derivatives was examined with an MTT assay with HeLa and L929 cells.[45,46] The impact of the structural modifications on the cell viability after a 24-h incubation of HeLa cells with starting CH and its derivatives solutions is presented in Figure 7. In general, it has been shown that the hydrophobic modification of CH does not significantly affect the cytocompatibility, especially for derivatives grafted with zwitterionic groups[47] or poly(ethylene glycol).[48] The derivatives were nontoxic to HeLa cells, and the viabilities remained around 90% regardless of DS_{Dod}. However, the zwitterionic derivatives (SPP_{36}–CH_L and SPP_{50}–CH_M) were more cytotoxic to the L929 cells than to the HeLa cells, and the viability decreased from 90% at 0.02 g/L to about 50% at 1.0 g/L. On the other hand, the dodecylated derivatives were less cytotoxic, and the viabilities for the L929 cells were similar to those exhibited by HeLa and remained around 80% (Figure S5, Supporting Information). Overall, the results confirm that the zwitterionic derivatives had good cytocompatibility and potential for pharmaceutical applications.

CONCLUSIONS

Zwitterionic CHs were synthesized by the Michael addition reaction with SPP followed by grafting with D_{CHO}. The insertion of zwitterionic groups onto the CH backbone provided water solubility over the entire pH range, and derivatives grafted with appropriate proportions of dodecyl groups formed spherical aggregates by self-assembly. At pH 7.4, the amphiphilic aggregates exhibited a high stability in aqueous solution; this was provided by the hydrophilic shell of the zwitterionic groups. We found that the derivatives with lower hydrophobe contents (2–5%) were more appropriate for obtaining nanosized

spherical particles, and regardless of the composition, the results from the MTT assay showed that all of the derivatives exhibited good cytocompatibility. These zwitterionic systems are under current investigation by our research group and may be promising carriers for drug delivery and gene therapy.

ACKNOWLEDGMENTS

This work was supported by the Conselho Nacional de Desenvolvimento Científico e Tecnológico (contract grant number 407499/2013-0). One of the authors (H. F. G. B.) is thankful to N. L. Bueno and J. Ruggiero from the Physics Department for their assistance with the DLS measurements. The authors are also thankful to C. C. S. Cavalheiro and A. Lima P. Neves from the University of São Paulo for allowing them access to the GPC equipment.

REFERENCES

1. Larsson, M.; Huang, W.-C.; Hsiao, M.-H.; Wang, Y.-J.; Nyden, M.; Chiou, S.-H.; Liu, D.-M. *Prog. Polym. Sci.* **2013**, *38*, 1307.
2. Desbrieres, J.; Martinez, C.; Rinaudo, M. *Int. J. Biol. Macromol.* **1996**, *19*, 21.
3. Du, Y.-Z.; Wang, L.; Yuan, H.; Wei, X.-H.; Hu, F.-Q. *Colloids Surf. B* **2009**, *69*, 257.
4. Duan, J.; Mansour, H. M.; Zhang, Y.; Deng, X.; Chen, Y.; Wang, J.; Pan, Y.; Zhao, J. *Int. J. Pharm.* **2012**, *426*, 193.
5. Guan, M.; Zhou, Y.; Zhu, Q.-L.; Liu, Y.; Bei, Y.-Y.; Zhang, X.-N.; Zhang, Q. *Nanomed. Nanotechnol.* **2012**, *8*, 1181.
6. Abbasi, S.; Yousefi, G.; Firuzi, O.; Mohammadi-Samani, S. *J. Appl. Polym. Sci.* **2016**, *133*, 43233.
7. Majedi, F. S.; Hasani-Sadrabadi, M. M.; VanDersarl, J. J.; Mokarram, N.; Hojjati-Emami, S.; Dashtimoghadam, E.; Bonakdar, S.; Shokrgozar, M. A.; Bertsch, A.; Renaud, P. *Adv. Funct. Mater.* **2014**, *24*, 432.
8. Zhao, S.-H.; Wu, X.-T.; Guo, W.-C.; Du, Y.-M.; Yu, L.; Tang, J. *Int. J. Pharm.* **2010**, *393*, 272.
9. Liu, W. G.; Zhang, X.; Sun, S. J.; Sun, G. J.; De Yao, K.; Liang, D. C.; Guo, G.; Zhang, J. Y. *Bioconjugate Chem.* **2003**, *14*, 789.
10. Zhu, D.; Jin, X.; Leng, X.; Wang, H.; Bao, J.; Liu, W.; Yao, K.; Song, C. *Int. J. Nanomed.* **2010**, *5*, 1102.
11. Chen, H.; Zhao, Y.; Cui, S.; Zhi, D.; Zhang, S.; Peng, X. *J. Appl. Polym. Sci.* **2015**, *132*, 42469.
12. Kurita, K.; Ikeda, H.; Yoshida, Y.; Shimojoh, M.; Harata, M. *Biomacromolecules* **2002**, *3*, 4.
13. Nishimura, S. I.; Miura, Y.; Ren, L. D.; Sato, M.; Yamagishi, A.; Nishi, N.; Tokura, S.; Kurita, K.; Ishii, S. *Chem. Lett.* **1993**, *22*, 1626.
14. Jiang, M.; Wang, K.; Kennedy, J. F.; Nie, J.; Yu, Q.; Ma, G. *Int. J. Biol. Macromol.* **2010**, *47*, 699.
15. Xu, Y. M.; Du, Y. M.; Huang, R. H.; Gao, L. P. *Biomaterials* **2003**, *24*, 5015.
16. Zhang, A.; Ding, D.; Ren, J.; Zhu, X.; Yao, Y. *J. Appl. Polym. Sci.* **2014**, *131*, DOI: 10.1002/app.39890.
17. Alves, N. M.; Mano, J. F. *Int. J. Biol. Macromol.* **2008**, *43*, 401.
18. Sahoo, S.; Sasmal, A.; Nanda, R.; Phani, A. R.; Nayak, P. L. *Carbohydr. Polym.* **2010**, *79*, 113.
19. Hu, F.-Q.; Meng, P.; Dai, Y.-Q.; Du, Y.-Z.; You, J.; Wei, X.-H.; Yuan, H. *Eur. J. Pharm. Biopharm.* **2008**, *70*, 757.
20. Mourya, V. K.; Inamdar, N. N. *React. Funct. Polym.* **2008**, *68*, 1051.
21. Yang, W.; Xue, H.; Li, W.; Zhang, J.; Jiang, S. *Langmuir* **2009**, *25*, 11916.
22. Sui, W.; Wang, Y.; Dong, S.; Chen, Y. *Colloids Surf. A* **2008**, *316*, 175.
23. Xu, P.; Bajaj, G.; Shugg, T.; Van Alstine, W. G.; Yeo, Y. *Biomacromolecules* **2010**, *11*, 2358.
24. Byeon, J. H.; Kulkarni, A.; Kim, H.-K.; Thompson, D. H.; Roberts, J. T. *Biomacromolecules* **2014**, *15*, 2320.
25. Meng, S.; Liu, Z.; Zhong, W.; Wang, Q.; Du, Q. *Carbohydr. Polym.* **2007**, *70*, 88.
26. Zeng, R.; Fu, H.; Zhao, Y. F. *Macromol. Rapid Comm.* **2006**, *27*, 552.
27. Zhu, A. P.; Shan, B.; Yuan, Y. L.; Shen, J. *Polym. Int.* **2003**, *52*, 85.
28. Liu, X.; Huang, H.; Liu, G.; Zhou, W.; Chen, Y.; Jin, Q.; Ji, J. *Nanoscale* **2013**, *5*, 3982.
29. Tiera, M. J.; Qiu, X.-P.; Bechaouch, S.; Shi, Q.; Fernandes, J. C.; Winnik, F. M. *Biomacromolecules* **2006**, *7*, 3156.
30. Hsiao, M.-H.; Tung, T.-H.; Hsiao, C.-S.; Liu, D.-M. *Carbohydr. Polym.* **2012**, *89*, 639.
31. Liu, G.; Luo, Q.; Gao, H.; Chen, Y.; Wei, X.; Dai, H.; Zhang, Z.; Ji, J. *Biomater. Sci.* **2015**, *3*, 499.
32. Sashiwa, H.; Yamamori, N.; Ichinose, Y.; Sunamoto, J.; Aiba, S. *Biomacromolecules* **2003**, *4*, 1254.
33. Philippova, O. E.; Volkov, E. V.; Sitnikova, N. L.; Khokhlov, A. R.; Desbrieres, J.; Rinaudo, M. *Biomacromolecules* **2001**, *2*, 490.
34. Tiera, M. J.; Tiera, V. A. D.; de Toledo, E. C.; de Sena, G. L. *Colloid Polym. Sci.* **2000**, *278*, 1060.
35. Moczek, L.; Nowakowska, M. *Biomacromolecules* **2007**, *8*, 433.
36. Philippova, O. E.; Korchagina, E. V. *Polym. Sci. Ser. A* **2012**, *54*, 572.
37. Schatz, C.; Pichot, C.; Delair, T.; Viton, C.; Domard, A. *Langmuir* **2003**, *19*, 9903.
38. Du, N.; Song, R.; Zhu, X.; Hou, W.; Li, H.; Zhang, R. *Chem. Commun.* **2014**, *50*, 10576.
39. Kim, Y. H.; Gihm, S. H.; Park, C. R.; Lee, K. Y.; Kim, T. W.; Kwon, I. C.; Chung, H.; Jeong, S. Y. *Bioconjugate Chem.* **2001**, *12*, 938.
40. Esquenet, C.; Terech, P.; Boue, F.; Buhler, E. *Langmuir* **2004**, *20*, 3592.

41. Korchagina, E. V.; Philippova, O. E. *Biomacromolecules* **2010**, *11*, 3466.
42. You, J.; Hu, F.-Q.; Du, Y.-Z.; Yuan, H. *Biomacromolecules* **2007**, *8*, 2456.
43. Liu, C. G.; Desai, K. G. H.; Chen, X. G.; Park, H. J. *J. Agr. Food Chem.* **2005**, *53*, 441.
44. Liu, C. G.; Chen, X. G.; Park, H. *J. Carbohydr. Polym.* **2005**, *62*, 298.
45. Wang, X.; Sun, X.; Jiang, G.; Wang, R.; Hu, R.; Xi, X.; Zhou, Y.; Wang, S.; Wang, T. *J. Appl. Polym. Sci.* **2013**, *128*, 3289.
46. Wang, J.-W.; Chen, C.-Y.; Kuo, Y.-M. *J. Appl. Polym. Sci.* **2011**, *121*, 3531.
47. Wu, M.; Dong, H.; Guo, K.; Zeng, R.; Tu, M.; Zhao, J. *Carbohydr. Polym.* **2015**, *121*, 121.
48. Zhu, S.; Qian, F.; Zhang, Y.; Tang, C.; Yin, C. *Eur. Polym. J.* **2007**, *43*, 2253.